Rapid molecular screening of black carbon (biochar) thermosequences obtained from chestnut wood and rice straw: A pyrolysis-GC/MS study

Kaal, Joeri ; Schneider, Maximilian P W ; Schmidt, Michael W I

DOI: https://doi.org/10.1016/j.biombioe.2012.05.021

Rapid molecular screening of black carbon (biochar) thermosequences obtained from chestnut wood and rice straw: A pyrolysis-GC/MS study

Joeri Kaal [a,*], Maximilian P.W. Schneider [b] and Michael W.I. Schmidt [b]

[a] Instituto de Ciencias del Patrimonio (Incipit), Consejo Superior de Investigaciones Científicas (CSIC), San Roque 2, 15704 Santiago de Compostela, Spain.

[b] University of Zurich, Department of Geography, 8057 Zurich, Switzerland.

* Corresponding author. Tel: +34 981563100 x 13588; fax: +34 981547104.

E-mail address: joeri.kaal@incipit.csic.es

Abstract

Rice straw and chestnut wood were heated between 200 and 1000 °C (T_{CHAR}) to produce Black C 'thermosequences'. The molecular properties of the charred residues were assessed by pyrolysis-GC/MS to investigate the relation between charring intensity and pyrolysis fingerprint. Samples obtained at T_{CHAR} > 500 ºC (wood) or > 700 ºC (straw) gave low quality pyrograms and poor reproducibility because of high thermal stability, but pyrolysis-GC/MS allowed to track the thermal degradation of the main biocomponents (polysaccharides, lignin, methylene chain-based aliphatics, triterpenoids, chlorophyll and proteins) in the lower temperature range, mostly occurring between T_{CHAR} 250 and 500 ºC. With increasing T_{CHAR}, the charred residues of these biocomponents lose characteristic functional groups, aromatise and finally condense into non-pyrolysable biomass. The proportions of the pyrolysis products of unspecific origin (benzene, toluene, PAHs, etc.), increase with charring intensity, while the ratios that reflect the abundance of alkyl cross-linkages between aromatic moieties (e.g. benzene/toluene, naphthalene/alkylnaphthalene) decrease. These results provide the guidelines to using pyrolysis-GC/MS for the molecular characterisation of different components in Black C and biochar, which is an important parameter for predicting Black C/biochar behaviour in soil. Results are consistent with earlier studies of these samples using the BPCA (benzenepolycarboxylic acid) method and the ring current-induced ^{13}C-benzene chemical shift NMR (Nuclear Magnetic Resonance) approach. Pyrolysis-GC/MS provides more information on molecular structures in the low temperature range ($T_{CHAR} \leq$ 500 ºC) while the BPCA and NMR ring current methods provide more reliable estimations of charring intensity, especially at higher temperatures ($T_{CHAR} \geq$ 500 ºC).

Keywords: Black C; biochar; Castanea sativa; Oryza sativa; charring degree; pyrolysis-GC/MS

1. Introduction

Thermally modified biomass, i.e. Black C (BC) or biochar, is increasingly being amended to cultivated soil to enhance soil fertility, reduce soil degradation and mitigate greenhouse gas accumulation into the atmosphere through C sequestration [1-4]. Nonetheless, the behaviour of BC in the soil environment depends on a large array of intrinsic BC properties (e.g. feedstock characteristics, charring temperature and duration, particle size) and soil conditions (moisture content, pH,composition and activity of the microbial population, parent material, etc.), which are only superficially understood [5-13].

One of the key parameters in predicting BC degradation/ preservation in soil is the degree of thermal alteration (charring intensity). Black C envelopes, with increasing charring intensity, weakly charred biomass, charcoal, soot and graphitic BC [14-16], which creates the so-called 'BC combustion continuum'. At the high-temperature end, BC consists of a strongly polycondensed (graphitic) aromatic network lacking most functional groups present in non-charred biomass. On the low temperature end, weakly charred biomass often contains chemical building blocks that reflect the biocomponent from which they originate, such as methoxyphenolic moieties from lignin and furan-like structures from carbohydrates [17-19]. As each biocomponent thermally rearranges at different temperatures, they form individual 'combustion continua'. As a result, recalcitrant and labile phases often coexist in a BC specimen [20]. Typically, with increasing charring intensity the C content, degree of condensation, specific surface area and sorption capacity of BC increase [21], while its susceptibility to degradation decreases [22-25].

Pyrolysis-GC/MS is one of the techniques available for studying the molecular properties of organic matter. It has been applied to BC previously [26-31], and the relationship between pyrolysis fingerprint and BC degradability was recently demonstrated by incubation studies [32-33]. Nonetheless, detailed interpretations of the data generated are scarce, especially using a relatively high pyrolysis temperature (700-750 ºC) that is considered more suitable for BC [17, 34-35]. The main objective of the present study is to (i) determine the thermal degradation of the compound groups present in ligno-cellulosic biomass (rice straw and chestnut wood) at temperatures that cover the range of both natural fires as well as common biochar preparation conditions (200-1000 ºC). These feedstocks and corresponding chars were studied previously by the benzene polycarboxylic acid (BPCA) method [36] and solid-state ^{13}C Direct Polarisation Nuclear Magnetic Resonance (^{13}C DP NMR) in combination with polycondensed aromatic ring current-induced chemical shift modification of bound ^{13}C benzene ("ring current NMR") [37]. Moreover, rice straw-derived BC/biochar has a large potential for C sequestration in rice-based systems yet knowledge on its molecular properties is scarce [13, 38-39]. The detailed description of the pyrolysis-GC/MS results aims to serve as a guideline for the assessment of the molecular properties of BC using this technique.

2. Materials and Methods

Chestnut (*Castanea sativa*) wood and rice (*Oryza sativa* Arborio) straw chars were prepared according to the protocol described in Hammes et al. [40]. Debarked and cut biomass was placed in a Carbolite CTF 16/75 furnace under N_2 flow (13 L h^{-1}) and the temperature raised from room temperature to 200 ºC at a rate of 300 ºC h^{-1} and then to

250-1000 ºC at a rate of 50 ºC h^{-1} to produce the chestnut wood and rice straw thermosequences. The final temperature (T_{CHAR}) was held constant for 5 h to assure complete charring, followed by a cooling period of 8 h after which the charred residues were collected. Samples were weighed before and after heat treatment to determine mass loss. The thermosequences originally included reference wood and grass chars of the Black Carbon Steering Committee [41] obtained at 450 ºC, which were described by Hammes et al. [40, 42], and studied by [28] and [30] using pyrolysis-GC/MS. However, these reference materials produced disparate results in the thermosequence, probably due to differences in feedstock particle size [36, 43, this study], and the corresponding pyrolysis-GC/MS results are therefore provided as Supplementary Material (S1). Samples are referred to as WX00 (chestnut; wood chars) and GX00 (rice; grass chars), with X00 indicating T_{CHAR}. Table 1 provides mass recovery after charring and the elemental composition of the residues.

Work by Keiluweit et al. [44] showed that wood and grass feedstocks charred at 200 ºC showed no chemical changes by FTIR and a weight loss of only 3%, and the cellulose remained virtually unaltered until 225 ºC charring as detected by a wide array of methodologies including pyrolysis-GC/MS, suggesting that the G200 and W200 pyrolysates can be considered as representative of the feedstock.

Pyrolysis-GC/MS was performed according to Kaal et al. [34]. Briefly, 1-1.5 mg of sample was placed in fire-polished quartz tubes with quartz wool on both ends and pyrolysed using a CDS Pyroprobe 5000 Pt coil filament instrument for 10 s at 750 ºC. Pyrolysis products were swept into a 6890N gas chromatograph (Agilent Technologies) by He flow (1 cm^3 min^{-1}), separated on a HP-5MS polysiloxane-based column

(temperature program 50–325 ºC at 20 ºC min^{-1}) and identified using an Agilent 5975B mass spectrometer operating in 70 eV electron impact mode. Quantification of pyrolysis products was based on the peak area of dominant and/or characteristic fragment ions. The relative abundances of each pyrolysis product were calculated as the percentage of the sum of all peak areas (total quantified peak area, TQPA). This is a semi-quantitative exercise that allows better recognition of differences between samples than visual inspection of pyrograms alone. Supplementary Material (S1) contains the background dataset, including pyrolysis product identifications, corresponding ion fragments, retention times and the relative contributions (% TQPA).

3. Results and Discussion

3.1 Pyrolysis-GC/MS

3.1.1 Total Quantified Peak Area (TQPA)

The pyrolysis products quantified cover the major peaks in the pyrograms, which implies that TQPA provides a rough estimation of signal intensity. In the present study, signal intensity is controlled by the pyrolysability of the material analysed [45]. Because the signal intensity of the chestnut wood chars obtained at $T_{CHAR} \geq 600$ ºC and rice straw chars at $T_{CHAR} \geq 800$ ºC was too low for meaningful quantification, in combination with poor reproducibility, we report only the results for chars obtained at $T_{CHAR} \leq 500$ ºC and $\leq$ 700 ºC for chestnut wood and rice straw, respectively. Fig. 1 shows that there is an exponential decrease in signal intensity with increasing T_{CHAR} for both feedstocks (wood, $r^2 = 0.96$; $P < 0.001$; grass $r^2 = 0.94$, $P < 0.001$), reflecting the increasing proportion of a polycondensed aromatic network that largely remains stable during analytical pyrolysis at

750 ºC. Lower TQPA values between T_{CHAR} 250 and 500 ºC suggests that chestnut wood tends to degrade and condense faster into such polycyclic aromatic domains than rice straw, which is in agreement with previous studies comparing wood and grass-derived BC [11, 36, 42].

The following sections discuss the pyrolytic behaviour of the main compound groups, in order of decreasing contribution to the T_{CHAR} 200 ºC pyrolysates: carbohydrates, lignin, methylene chain compounds, N-containing pyrolysis products, chlorophyll and steroids/triterpenoids; followed by the pyrolysis products of unspecific origin: monocyclic and polycyclic aromatic hydrocarbons (MAHs/PAHs), phenols, other O-containing aromatic compounds and finally a set of unidentified compounds.

3.1.2 Carbohydrates

The contribution of carbohydrate products in W200 is ca. 68 % while that of G200 is 35 % of TQPA (Fig. 2a). In addition, there are differences between the main carbohydrate products from W200 and G200: while W200 produced mainly 1,6-anhydro-β-D-glucopyranose (levoglucosan), 3/2-furaldehyde and 1,4:3,6-dianhydro-α- D -glucopyranose, G200 produced predominantly furanones, 3/2-furaldehyde and acetic acid. This may be explained by (1) differences in polysaccharide composition, with the high levoglucosan contribution from glucose units in cellulose in chestnut wood against the relatively high proportion of acetic acid and furanones from pentose moieties (e.g. xylose) and uronic acids in hemicelluloses in rice straw [46-47] or (2) significantly reduced levoglucosan yield upon cellulose pyrolysis in G200 because of higher ash content [48]. Note that from elemental analysis, estimated ash content of the chestnut

wood and corresponding chars is negligible (< 2 mg g^{-1}) while that of rice straw increases from 85 mg g^{-1} (T_{CHAR} 200 ºC) to 170–220 mg g^{-1} (T_{CHAR} 400-1000 ºC). Analogously, enhanced base-catalysed decomposition of levoglucosan and inhibited intramolecular condensation (transglycosylation) were observed to have a significant effect on pyrolysis fingerprints of K-impregnated cellulose [49].

For chestnut wood, the proportion of carbohydrate markers decreases rapidly from 68 % towards 20 % of TQPA between T_{CHAR} 250 ºC and 300 ºC. This change is indicative of the early loss of carbohydrates upon heat treatment, which is in agreement with significant weight loss (Table 1) and existing knowledge on thermal rearrangement of polysaccharides in this temperature range [5, 17, 50-52]. Furthermore, analogous to pyrolysis studies of charred cellulose by Pastorova et al. [17], the contribution of 1,6-anhydrosugars, including levoglucosan, from chestnut wood chars diminishes from 60 % to < 5 % of the sum of carbohydrate markers between W250 and W300 (Fig. 2b). This process is indicative of the thermal rearrangement of the residual carbohydrate fraction into a weakly-charred partially non-hydrolysable carbohydrate residue that does not undergo transglycosylation during analytical pyrolysis [20], probably because of depolymerisation during heat treatment. This coincides with a relative increase in the proportion of furan-based pyrolysis products between T_{CHAR} 250 and 350 ºC (Fig. 2c). The initial shift from anhydrosugars to furan-like compounds in pyrolysates was also detected by Almendros et al. [53] using cellulose char (350 ºC for 3 min under oxidative conditions). For W500, less than 2 % of TQPA could be tentatively assigned to carbohydrate pyrolysis products (mostly benzofurans; Fig. 2d), mainly originating from strongly charred carbohydrates. For the rice straw chars, a similar negative trend in

relative proportion of carbohydrate pyrolysis products with increasing T_{CHAR} is observed, namely from 35 % of TQPA in G200 towards 2 % in G500.

In summary, for both species the general trend in dominant carbohydrate products is from 1,6-anhydrosugars, pyrans and some of the furans and cyclopentenones ($T_{CHAR} \leq 250$ ºC) towards a clear prevalence of furans, furanones, cyclopentenones, furfurals and a bifuran compound (T_{CHAR} 300-350 ºC) and finally benzofurans and dibenzofurans (and undoubtedly also an unknown portion of the unspecific aromatic and phenolic products, see below) at $T_{CHAR} > 350$ ºC. The vast majority of environmental BC samples do not produce the compounds in the first group (1,6-anhydrosugars and pyrans), and their identification in pyrolysates should be considered indicative of the presence of uncharred or very weakly charred biomass. Such material is often found in the interior part of charcoal particles [54] and is eliminated from charcoal rapidly after incorporation into soil [34]. The detection of furan and benzofuran moieties in ^{13}C NMR studies of charred carbohydrates [5, 55] suggests that the corresponding pyrolysis products actually originate from such moieties (i.e., they are not merely secondary pyrolysis rearrangement products). Kaal and Rumpel [56] suggested that the benzofuran/C_1-benzofuran is a useful parameter for estimating charring intensity but, even though this ratio does increase strongly at $T_{CHAR} > 400$ ºC, there is no consistent trend below that temperature.

3.1.3 Lignin

Upon pyrolysis, both W200 and G200 produced large amounts of methoxyphenols (guaiacols and syringols), which originate from lignin (Fig. 3a). For chestnut wood chars W275 and W300, the sum of lignin markers show a maximum because of the degradation of the relatively thermolabile carbohydrates in this

temperature range. At T_{CHAR} 350 ºC the contribution of the lignin markers declines towards < 5 % in both W350 and G350, and they are below the detection limit at $T_{CHAR} \geq$ 400 ºC. These results reflect the demethylation and/or demethoxylation of lignin [56]. Thus, at $T_{CHAR} \geq$ 400 ºC, lignin cannot be identified unambiguously anymore.

Guaiacols and syringols with a C_3 side chain originate from lignin moieties with mostly intact propylene side chains and β-O-4 cross-linkages between aromatic building blocks [57]. The relative proportions of these pyrolysis products with respect to their non-C_3-guaiacol and -syringol analogues, i.e. C_3G/G and C_3S/S, decline with increasing T_{CHAR}, mainly between 200 and 300 ºC (Fig. 3b- and c), which is indicative of side chain elimination and probably also depolymerisation of lignin. This is in agreement with the pyrolysis fingerprints of charred gorse wood [31]. The syringols-to-guaiacols (S/G) ratio declines with increasing T_{CHAR} for both biomass sources (Fig. 3d) as well. This does not necessarily imply that syringyl lignin is thermally more labile than guaiacyl lignin, as demethoxylation of syringol units into guaiacol units is likely to occur during charring of syringyl lignin [31]. The C_3G/G, C_3S/S and S/G ratios are common parameters in identifying source material and estimating the degradation state of lignin in peat deposits and soils [58]. Therefore, these parameters are not useful for identifying charred lignin or for estimating its degree of charring from BC-containing soil organic matter admixtures in environmental samples, but for fresh laboratory-produced BC/biochar these methoxyphenolic pyrolysis products and the aforementioned parameters do allow for the detection of weakly-charred or uncharred lignin, which is an important parameter in biochar lability estimation [32]. On the other hand, for palaeo-environmental analysis,

these indicators of source or degradation state of lignin or lignin-derived moieties should be handled cautiously if the possibility of burning is not ruled out.

3.1.4 Methylene chain compounds

The methylene chain compounds is a group of 130 quantified pyrolysis products which contain linear aliphatic chains of more than three carbon atoms, most of which accounting for only minor proportions of TQPA. This group consists of homologous series of C_{11}-C_{33} alkanes, $C_{11:1}$-$C_{31:1}$ alkenes, C_{12}-C_{18} fatty acids (FAs), C_{15}-C_{31} fatty acid methyl esters (FAMEs), C_4-C_{25} alkylbenzenes and branched *n*-alkanes (probably C_{12}-C_{19}). Furthermore, C_{21} methylketone, C_9 and C_{14} alkylcyclopentane, C_8-C_{16} alkylcyclohexanes and alkenylcyclohexanes, and a set of eight probably branched *n*-alkane fragments that appeared scattered in the domain of the short-chain aliphatic compounds (probably C_8-C_{11}). The sum of the methylene chain compounds is higher in grass chars than in wood chars (Fig. 4a), probably because they originate largely from epidermal plant cuticles. For wood chars, their contribution increases from W200 (0.2 % of TQPA) to W300 (5.9 %) and then declines to 0.2 % in W500. For grass chars, in G200 the contribution is 3 %, increases to 37 % at G400, and then declines to 13 % at G700. The initial increase with $T_{CHAR} \leq 300$ ºC (wood) or ≤ 400 ºC (grass) can be explained by preferential thermal degradation of other biocomponents, especially carbohydrates [19]. The presence of methylene chain compounds in higher temperature chars are indicative of the thermal resilience of their precursors in comparison with the other main components in lignocellulosic feedstocks [45].

Wood chars produced only very small amounts of FAs (C_{16} and C_{18}), which declined from 0.02 % of TQPA in W200 to 0.002 % at W300, and could not be distinguished from the noise background at higher temperatures (Fig. 4b). The grass chars, on the other hand, produced more FAs upon pyrolysis, in the C_{12}-C_{18} range. Their sum decreased from 0.8 % (G200) to 0.2 % (G300), and could not be detected at higher temperatures. The FAs in pyrolysates are often considered evaporation rather than pyrolysis products [59].

The straight chain *n*-alkanes and *n*-alkenes account for 53 ± 27 % of the methylene chain compounds (Fig. 4c). The *n*-alkanes and *n*-alkenes combined account for 0.1 % of TQPA in W200 and 1.3 % in G200. Maximum contributions are found in W300 (1.1 % of TQPA) and G400 (30.3 % of TQPA), after which their contributions tend to decline (0.2 % in W500 and 1.1 % in G200). Average chain length shortening of both *n*-alkanes and *n*-alkanes upon increasing T_{CHAR} are evident for both feedstocks, from 20 to ca. 15 for wood chars and from ca. 21 to 13 for grass chars (S1), which was also observed by [18,19,60]. For rice straw chars, heat-induced *n*-alkane chain length shortening is most evident between T_{CHAR} 400 ºC (20.1) and T_{CHAR} 500 ºC (14.6).

For the first time a series of cyclic aliphatic compounds were detected in BC pyrolysates, viz. *n*-alkylcyclopentanes, *n*-alkylcyclohexanes and *n*-alkenylcyclohexanes. For the chestnut wood chars, the sum of these alkylcyclocompounds is highest in W300 (0.1 % of TQPA), against 2.2 % at G500 for rice straw (Fig. 4d).

Both feedstocks produced most of the FAMEs in the C_{15}-C_{31} range. Chars obtained at $T_{CHAR} \geq 300$ ºC generally lacked the long-chain (C_{20}-C_{31}) FAMEs (S1).

FAMEs have their maximum contribution in W275 (0.1 % of TQPA) and G275 (0.4 %) and the average chain length declines from ca. 19 to 17 between T_{CHAR} 300 and 350 ºC.

An arbitrary distinction is made between C_1-C_3 alkylbenzenes (see MAHs Section 3.1.8) and C_4-C_{25} alkylbenzenes, because the first group may originate from cyclisised aliphatics but also lignin precursors while the second group may be safely expected to originate exclusively from aliphatic precursors. The C_4-C_{25} alkylbenzenes probably originate from cyclisised linear methylene chain compounds during experimental charring, although a small proportion of these *n*-alkylbenzenes detected in the T_{CHAR} < 350 ºC rice straw chars may originate from FAs cyclisised during analytical pyrolysis as well [61]. Their contribution to TQPA is higher in the rice straw than in the chestnut wood chars, and increases from 0.0 % (W200) to 0.6 % (W350) and from 0.3 % (G200) to 4.8 % (G400) (Fig. 4e). At higher temperatures, their contribution declines. Average chain length of the alkyl side chain declines from 15 to 7 in between T_{CHAR} 200 ºC and T_{CHAR} 500 ºC for the chestnut wood chars, and from 8 (T_{CHAR} 350 ºC) to 5 (T_{CHAR} 700 ºC) for the rice straw chars. Small peaks of *n*-alkylbenzenes with unsaturated side chain (also producing *m*/*z* 91 and 92) might have interfered in the C_{16}-C_{25} alkylbenzenes range, but these will not have affected the interpretations giving here.

A set of short-chain *n*-alkane fragments (m/z 57) eluted between 6.7 and 8.2 min (probably a set of branched compounds within the C_8-C_{11} range) was abundant especially in high-temperature chars from rice straw (Fig. 4f). In G350, this contribution is already 1.1 % of TQPA, and increases steadily to almost 10 % of TQPA at T_{CHAR} 700 ºC. These compounds, of unknown molecular structure, reflect the presence of a relatively thermostable aliphatic rearrangement product.

Branched *n*-alkanes, probably C_{12}-C_{19}, accounted for 0.1-0.2 % of TQPA in W350 and W400, and 0.1-1.7 % for the grass chars (maximum for G500) (S1). In the grass chars, the contribution of these compounds increases with increasing T_{CHAR} up until T_{CHAR} 500, after which it declines. Samples W250 and W300 produced significant amounts of branched C_{12}-C_{19} alkenes (0.6 % and 4.5 % of TQPA, respectively), not detected in any other samples.

The only *n*-methylketone compound that could be quantified was C_{21} methylketone, which was only detected in grass char pyrolysates. Its contribution to TQPA increases from 0.01 % to 0.09 % between G200 and G250, and disappears at T_{CHAR} $\geq$ 350 ºC (S1).

Processes behind these trends are most likely (1) decarboxylation or volatilisation of free FAs, (2) chain length shortening, (3) cyclisation, (4) aromatization and (5) branching/recombination. The final polyaromatisation step, possibly in part reflected by alkyl-PAHs, cannot be recognised because these PAHs do not originate exclusively from methylene chain precursors (Section 3.1.8). These results are in striking agreement with Wiesenberg et al. [19] who studied total lipid extracts from grass straws charred at 300-500 ºC using GC/MS, suggesting that the branching, chain length shortening and aromatisation reactions, as reflected by pyrolysis-GC/MS of the thermosequences studied here, occur mostly during the experimental heating and not artificially during analytical pyrolysis.

3.1.5 Nitrogen-containing pyrolysis products

The N-containing compounds detected are pyrroles (pyrrole, C_1-pyrrole, diketodipyrrole), pyridines (pyridine and C_1-pyridines), benzonitriles (only benzonitrile was quantified) and C_{16}-C_{20} alkylamides (saturated and mono-unsaturated, in rice straw char pyrolysates from T_{CHAR} 200 to 300 only). All N-containing pyrolysis products are more abundant in the rice straw chars, which has a higher N content (Table 1). In the rice straw chars, an initial increase (G200-G275) in the sum of N-containing pyrolysis products (Fig. 5a) can be explained by carbohydrate degradation (preferential elimination of O over C and N), followed by a decline at $T_{CHAR} \geq 300$ ºC because of the loss of N functional groups in this range (corresponding to C enrichment), a trend that is frequently observed during heat treatment studies [44,62,63]. For the chestnut wood chars, the contribution of N-containing pyrolysis products increases until W400, suggesting that the N is incorporated in thermostable groups, probably heterocyclic aromatic moieties [64,65] even though a considerable contribution of recalcitrant amide N cannot be excluded [66]. As was observed previously [56], there is a general trend with increasing T_{CHAR} from pyrroles to pyridines to benzonitriles (Fig. 5b-d). The proportion of benzonitrile among the N-containing pyrolysis products increases more significantly in chestnut wood than in rice straw chars, which supports the aforementioned relatively fast rearrangement and condensation into thermostable fractions for chestnut wood.

3.1.6 Plant steroids (triterpenoids)

A series of products from plant steroids (steradienes and steratrienes) were detected in the pyrolysates of both feedstocks up until T_{CHAR} 300 ºC (S1). The sum of these compounds accounted for up to 0.03 % of TQPA in wood chars (W200) and up to

0.2 % of TQPA in grass chars (G275). None of these compounds could be detected after heating at $T_{CHAR} \geq 350$ ºC, which is in agreement with [19]. The initial increase in the proportion of these triterpenoids in the rice straw chars suggests a slightly higher thermal stability of their precursor than that of the carbohydrates in rice straw feedstock.

3.1.7 Chlorophyll

A phytadiene compound was the only unequivocal pyrolysis product of chlorophyll. It originates from the pyrolytic cleavage and consequent dehydration of the phytyl side chain in chlorophyll a and b. This compound was only detected in the rice straw series, contributing 0.10 % to TQPA in G200 and 0.02 % in G300 (Fig. 6a). Similarly, prist-1-ene was not detected in the pyrolysates of chestnut wood chars, while it was detected in the grass char samples up until T_{CHAR} 500 ºC (Fig. 6b). Prist-1-ene is a product of the cleavage of ester-bound phytol [67]. In the present study, prist-1-ene most likely reflects the thermal degradation of phytol chains, giving rise to a decrease in the ratio phytadiene/prist-1-ene from 0.4 (G200) to 0.02 (G300) (S1), which was also observed by Ishiwatari et al. [68] using pyrolysis-GC/FID of preheated chlorophyll. The shift from phytadiene to prist-1-ene in pyrolysates does not necessarily reflect charring conditions, however, as this is also witnessed in peat and kerogen maturation studies and probably also chlorophyll degradation in soil. From an experimental exercise using pyrolysis-GC/MS of charred rye grass, González-Vila et al. [45] considered the pyrroles as chlorophyll products. However, according to their presence in the pyrolysates from chestnut wood chars, these compounds are more likely to originate largely from structural proteins in cell walls.

3.1.8 Monocyclic and polycyclic aromatic hydrocarbons (MAHs/PAHs)

The MAHs (benzene, toluene, C_2-benzenes and C_3-benzenes) form the most abundant group of source-unspecific aromatic products. These pyrolysis products are of little diagnostic value to identify source material and therefore frequently ignored in pyrolysis-GC/MS studies, even in BC studies in which they are often the most abundant pyrolysis products [28,69]. The MAHs account for 1.4 % of TQPA for W200 and 6.3 % in G200. These proportions increase strongly with increasing T_{CHAR} (Fig. 7a), reflecting the aromatisation and loss of functional groups mainly from lignin and carbohydrates. The benzene-to-toluene ratio, which was proposed as an indicator of the degree of charring of BC [56], increases significantly from T_{CHAR} 400 ºC onwards (Fig. 7b), but changes only slightly below T_{CHAR} 400 ºC, which limits the validity of this parameter in the low temperature domain.

The PAHs group consists of indene, C_1-indenes, naphthalene, C_1-C_3 alkylnaphthalenes, dihydronaphthalenes, biphenyl, fluorenes, C_1-biphenyls, phenanthrene, anthracene, pyrene, a pyrene isomer, dihydropyrene, diphenylmethane, naphthalenol and C_1-naphthalenol, a total of 30 pyrolysis products. The sum of these compounds increases with T_{CHAR} for chestnut wood and rice straw alike (Fig. 7c). However, many of these compounds increase only until T_{CHAR} 350-400 ºC, after which their contributions decline. In general, the PAHs lacking an alkyl group (non-alkylated PAHs such as naphthalene, biphenyl, fluorene and pyrene) continue increasing towards maximum T_{CHAR} values (Fig. 7d) while the alkylated PAHs (C_1-C_3 naphthalenes, C_1-biphenyls, etc.) decrease in the high temperature range (Fig. 7e). This process, reflected by the naphthalene/C_1 naphthalene ratio (which form the most frequently found PAH-

alkyl PAH pair in BC pyrolysates) was suggested to reflect the elimination of alkyl cross-linkages between aromatic clusters [19, 31, 56, 70]. This ratio increases more strongly at T_{CHAR} > 350 ºC (Fig. 7f).

3.1.9 Phenols

The phenols (phenol, C_1-C_3 alkylphenols, 4-formylphenol, 4-vinylphenol, catechol and C_1-catechol) form a significant yet difficult to interpret group of pyrolysis products, considering the many sources that produce phenols upon pyrolysis (lignin, carbohydrates, proteins, tannins, suberin, etc.). They tend to increase from T_{CHAR} 200 ºC to a maximum value at T_{CHAR} 300-350 ºC, where the phenols account for ca. 30-40 % of TQPA (Fig. 8a). Considering the nature of the source material (lignin-carbohydrate-dominated), most phenols would originate from demethylated and demethoxylated groups in lignin. This demethylation/demethoxylation of lignin, and an associated decrease in the methoxyphenol to phenol ratio, is a well-known effect of charring [31,45,71]. The proportion of phenol (Fig. 8b) and especially C_1-C_3 alkylphenols (Fig. 8c) declines rapidly at T_{CHAR} 500 ºC and higher, which represents lignin dehydroxylation possibly in combination with carbohydrate aromatisation. This process coincides with an increase in the contributions of MAHs and PAHs. Therefore, the thermal degradation of lignin can be summarised as follows: loss of C_3 side chains (reflecting depolymerisation and side-chain elimination), followed by demethylation/demethoxylation, dehydroxylation and finally incorporation into a polyaromatic network. Except for the final polycondensation reactions, these changes occur mostly below T_{CHAR} 500 ºC.

4-vinylphenol does not behave as the other phenols (Fig. 8d). This compound was not detected in the chestnut wood chars but accounted for a significant proportion of the G200 pyrolysate. The contribution of 4-vinylphenol decreases from 7.0 % of TQPA to 1.2 % for G300. At higher temperatures this compound cannot be detected anymore. 4-vinylphenol reflects intact coumaryl grass lignin and not, as most of the other phenols, a thermal demethylation product of methoxylic groups in guaiacyl- or syringyl-based lignin.

In the present study, catechol and C_1-catechol (S1) largely originate from either tannins or demethylated lignin [72,73]. For both wood and grass chars, their contribution to TQPA decreases from T_{CHAR} 200 to 275 ºC, show relatively high values at T_{CHAR} 300 ºC, and disappear in T_{CHAR} 350 or 400 ºC. The initial decrease may reflect the partial dehydroxylation of tannin, while the second maximum at T_{CHAR} 300 ºC may reflect a significant lignin source of these compounds. Even though chestnut wood is known for its high condensed tannin content [74], its catechol contributions are not markedly higher than that of rice straw pyrolysates. Nonetheless, catechol and pyrogallol pyrolysis products are poorly observed using a non-polar GC column, and the higher phenols contributions in W200 compared to G200 may be partially explained by the presence of tannins.

Buurman (pers. comm.) inferred that an homologous series of long-chain *n*-alkylphenols is characteristic of pyrolysates from charred biomass, but these compounds were not found in the present study.

3.1.10 Other oxygen containing aromatic compounds

A set of aromatic compounds with methoxyl or ketonic groups that are not frequently detected in the pyrolysates of lignin probably reflect some intermediate thermally rearranged lignin precursor. These compounds (C_1-methoxybenzene, a dimethoxytoluene, acetophenone, 3-methoxycatechol and two isomers of C_1-hydroxybenzaldehyde) all give small contributions at T_{CHAR} 200, maximise between T_{CHAR} 275 and 400 ºC and are not detectable at $T_{CHAR} \geq$ 400 (S1), which is in agreement with the interpretation of these compounds as intermediate lignin degradation products.

3.1.11 Other compounds

From their resemblance with mass spectral patterns published by Rushdi et al. [75], we tentatively identified two pyrolysis products producing *m*/*z* 105, 118, 264 and 382 and *m*/*z* 105, 118, 278 and 396 as *seco*-cholestatriene derivatives (S1). These products may have formed upon charring-induced fission of the B ring and subsequent aromatisation of the A ring of tetracyclic steroids. Their maximum contribution was found for G300 and these compounds cannot be detected at higher temperatures. Contrary to [19] for charred rice straws, monoaromatic pentacyclic triterpenoid derivatives were not detected.

β-tocopherol was only detected in the grass chars (G200-G300) (S1). D-limonene compounds which probably originate from cyclic terpenes were only detected in grass chars as well, up until T_{CHAR} 300 ºC. The other unidentified compounds produced fragment ions *m*/*z* 159 + 174 (possibly an indanone or tetrahydronaphthalene compound), *m*/*z* 97 (an unidentified polar substance), *m*/*z* 57 + 194 (unknown), *m*/*z* 177 + 220 and *m*/*z* 191 + 206 (possibly multi-substituted naphthalene-based compounds).

3.1.12 Concluding remarks of pyrolysis-GC/MS results

The relative proportions of the main pyrolysis product groups shows how the markers of the major components of the chestnut wood (Fig. 9a) and rice straw (Fig. 9b), i.e. carbohydrates and lignin, are degraded and replaced by markers of unspecific source (phenols, MAHs and PAHs) and aliphatic compounds (in rice straw chars). Despite of the diverse thermal degradation pathways and temperatures of the individual biocomponents, these general results would allow dividing the chars in three classes defined by Keiluweit et al. [44] according to the classification of laboratory-produced wood and grass chars: (i) "plant material largely unaffected by thermal treatment" (T_{CHAR} 200-250 ºC), with pyrolysis products typical of intact or weakly charred biocomponents, such as 1,6-anhydrosugars, pyrans, guaiacols, syringols, phytadienes and FAs, (ii) "transition chars" (T_{CHAR} 275-350 ºC), where pyrolysis products of thermally altered carbohydrates (e.g. furans), lignin (methoxyphenols), proteinaceous biomass, chlorophyll (pristene) and methylene chain-based components (e.g. *n*-alkanes/*n*-alkenes) can still be recognised and (iii) "amorphous char […] composed of small, heat-resistant aliphatic and (hetero) aromatic elements" (T_{CHAR} 400-500 ºC), in which pyrolysis products of unspecific origin dominate (MAHs, PAHs, phenols and some short-chain methylene compounds). The higher temperature (>500-700 ºC) phases consisting of graphitic structures cannot be identified using pyrolysis-GC/MS because of their thermal stability under the pyrolysis conditions applied here.

3.2 Comparing pyrolysis-GC/MS, the BPCA method and "ring current NMR"

These three techniques provide parameters for BC content as well as parameters for charring intensity of the BC. For pyrolysis-GC/MS, the sum of the most abundant BC products, i.e. Σ(MAHs, PAHs, benzonitrile), is a representative parameter of the relative proportion of BC [69]. This sum (Fig. 10a), which shows an increase with increasing T_{CHAR} from 2 % (W200) to 98 % (W500) and from 9 % (G200) to 85 % (G700) of TQPA for the chestnut wood and rice straw thermosequences, respectively, is used here for comparison with the BPCA and ^{13}C NMR ring current methods. The Σ(MAHs, PAHs, benzonitrile) parameter is semi-quantitative and does not provide BC concentrations. An additional disadvantage is that for samples with a considerable contribution of non-pyrogenic organic matter producing MAHs or PAHs upon pyrolysis, other parameters should be considered (e.g. using only the more specific markers of BC such as unsubstituted phenanthrene, anthracene and pyrene [29]). The main advantage of pyrolysis-GC/MS is the level of detail on the molecular structures present, for both BC as well as non-pyrogenic material.

Using the BPCA method, the Total BPCA-C yield is the quantitative measure for BC contents [36]. Total BPCA-C increases steadily from T_{CHAR} 200 to T_{CHAR} 500 ºC, after which it shows a decline (Fig. 10b). This represents gradual condensation of aromatic moieties until T_{CHAR} 500-600 ºC and finally incomplete oxidation of chemically resistant graphitic moieties at T_{CHAR} 700-1000 ºC [36]. Interference of non-pyrogenic material is of less importance for the BPCA method, so that the Total BPCA-C yield is a reliable and quantitative parameter.

McBeath et al. [37] applied the novel ring current NMR approach to the chestnut wood thermosequence. This method provides estimations of the % of BC (as % of

aromatic C signal in DP NMR spectra). The % of aromatic C shows a strong increase from 30 % at W200 to 75 % for W275 (reflecting the elimination of intact polysaccharides), followed by smaller increases towards 90 % for W400 (reflecting elimination of mainly lignin methoxyl) and 100 % for W600 (lignin hydroxyl elimination) (Fig. 10c). For ^{13}C NMR, interference of non-pyrogenic aromatic components (e.g. lignin) in the % of aromatic C strongly mitigates its potential to provide estimations of BC content, even though a molecular mixing model may partially solve this problem [56].

With respect to the parameters for estimating the charring intensity of BC, the pyrolysis-GC/MS indicators for the abundance of alkyl cross-linkages (benzene/toluene and naphthalene/C_1-naphthalene ratios, Fig. 7) show an increase at T_{CHAR} > 350 ºC. The temperature range for which these ratios provide an estimation of the charring intensity (ca. 350-500 ºC) is relevant but rather narrow.

Three BPCA-derived parameters have recently been suggested to describe the charring intensity of BC: (i) the concentration of B6CA (B6CA-C/Total C) [36], (ii) the proportion of B6CA among all BPCA (B6CA-C/Total BPCA-C) [21] and (iii) the average number of acidic groups in the BPCA (BμCA, ranging from 4 to 6) [76]. The first parameter (B6CA-C/Total C, not shown) is the only one that does not show almost constant values in the T_{CHAR} 250-500 ºC range (for chestnut wood) and T_{CHAR} 250-400 ºC (for rice straw), but has the obvious disadvantage that samples must be devoid of non-pyrogenic material. The other parameters, i.e. B6CA-C/Total BPCA-C (Fig. 10d) and BμCA (Fig. 10e), show largest incremental increases between T_{CHAR} 500 and 800 ºC, but

are insensitive for estimating the degree of charring in the lower temperature range (T_{CHAR} 250-400/500 ºC).

For the NMR ring current approach (data available for chestnut wood thermosequence only), an indication of the degree of thermal impact is calculated from the change in chemical shift of BC-bound ^{13}C benzene (-Δδ), which is based on electric ring currents induced by polyaromatic ring clusters. -Δδ of W200 is 0.0 ppm, is 0.3-0.8 ppm for W250-500 and 1.9-10.0 ppm for W500-W1000 (Fig. 10f), thus showing an exponential increase with increasing T_{CHAR}. Unsurprisingly, the -Δδ parameter is especially useful for characterising high-T chars while it is insensitive for the functional group elimination, aromatisation and initial condensation reactions (especially below 350 ºC). Using ab initio simulation of -Δδ for model PAHs, the authors estimated the size of the polyaromatic domains. These calculations indicated that in the low-T range (-Δδ < 0.6 ppm until W500) polyaromatic groups ≤ 3 rings dominate, whereas at T_{CHAR} 500 ºC aromatic domains no larger than coronene (7 ring PAH) prevail. The size of these domains increases rapidly in samples produced at T_{CHAR} > 700 °C, with predominantly clusters > 19 rings. Hence, -Δδ not only provides a reliable parameter of the charring intensity at T_{CHAR} > 300 ºC, it may additionally provide quantitative information on aromatic cluster size (more research is required to confirm this).

The difference between BC/biochar with a high or low proportion of labile C –i.e. labile against dichromate oxidation [77] or microbial degradation during incubations [13,33,78]– often lies in the T_{CHAR} 250-450 ºC range (‘transition’ and ‘amorphous’ chars), which implies that an important aspect of BC/biochar behaviour after soil amendment may be predicted by pyrolysis-GC/MS characterisation based on the abundance of BC

products vs. recognisable elements of the biocomponent types discussed earlier (Sections 3.1.2-3.1.7), yet with major quantitative limitations. The BPCA and ring current NMR methods may not be able to detect these changes because in this range the principal reactions involved are the loss of many functional groups combined with initial aromatisation, while polycondensation is minor.

It is concluded that for estimating BC content, the BPCA method is the most suitable method, while pyrolysis-GC/MS and ^{13}C DP NMR provide more qualitative parameters. For molecular characterisation of BC, pyrolysis-GC/MS provides the highest level of detail, at least until T_{CHAR} 400-500 ºC, but the BPCA method and ^{13}C DP NMR in combination with ring current NMR provide more consistent parameters for charring intensity of BC which are valid also for very high-T chars. Therefore, these methods provide complementary information, with BPCA and ring current NMR being more suitable for high T chars (≥ 400 ºC) and quantification, while pyrolysis-GC/MS is quantitatively weak but appropriate for detailed characterisation in the lower T range (≤ 500 ºC). This is not surprising, because the pyrolysability of BC relies on the abundance of pyrolysable cross-linkages (ether, ester, alkyl, etc.) between small aromatic clusters, while the BPCA and ring current NMR methods measure the degree of polycondensation, starting from aromatic clusters three rings in size [37,79]. Thus, larger clusters of polyaromatic domains (high T) can be assessed by the BPCA and ring current NMR methods but are resistant against pyrolysis, while smaller clusters and non-polycondensed portions of BC (low T) are amenable to pyrolysis-GC/MS but escape the analytical window of the BPCA and ring current NMR methods.

Today, pyrolysis-GC/MS is the least expensive technique. Analytically, the NMR ring current method and pyrolysis-GC/MS are less time-consuming than the BPCA method. On the other hand, the creation and interpretation of the pyrolysis-GC/MS dataset is more time-consuming and prone to operator-dependent bias than BPCA and NMR ring current methods data elaboration.

4. Conclusions

It appeared that with increasing heating temperature (T_{CHAR}), the major trends in pyrolysis fingerprint of chestnut wood and rice straw chars are an increase in (poly)aromatic pyrolysis products, branched and short-chain *n*-alkanes and benzonitrile, while the pyrolysis markers of lignin, polysaccharides, long-chain methylene chain-based components, triterpenoids and chlorophyll disappeared, mainly, but depending on biocomponent class, between T_{CHAR} 250 °C and 500 °C.

The major changes in the lignin signature are C3 side chain elimination (which promotes depolymerisation), demethylation of methoxylic groups, dehydroxylation and finally polycondensation. For carbohydrates even low-T charring causes a strong decline in the proportion of 1,6-anhydrosugars from intact cellulose in chestnut wood and several pentose markers from rice straw, and an increase in furans. Further charring causes a shift from furans to benzofurans, benzenes and PAHs. The straight-chain *n*-alkane/*n*-alkene pairs from uncharred lipids show progressive chain length shortening, then cyclisation and eventually (poly)aromatisation. With increasing degree of thermal impact the pyrolysis fingerprint of proteinaceous biomass shifts from pyrroles to pyridines to benzonitriles and polyaromatic nitriles. Chlorophyll product shift from phytadienes to

pristene between 250 °C and 300 °C and cannot be recognised in the pyrolysates of high-T chars.

Pyrolysis-GC/MS provides a rapid screening of the molecular properties of Black C or biochar specimen, which can be used to help predict its degradation/preservation behaviour in soil. Pyrolysis-GC/MS of BC is complementary to the quantitatively more reliable information offered by the BPCA molecular marker and ^{13}C NMR ring current methods.

Acknowledgements

This study was partly funded by the Spanish Ministry of Science and Education under the framework of the CONSOLIDER-INGENIO 2010 program TCP (CSD2007-00058). We wish to thank Anna McBeath for kindly providing us with ring current NMR data and Dr. R. Overend and an anonymous reviewer for their time and suggestions.

References

[1] Lehmann J, Liang B, Solomon D, Lerotic M, Luizão F, Kinyangi J, et al. Near-edge X-ray absorption fine structure (NEXAFS) spectroscopy for mapping nanoscale distribution of organic carbon forms in soil: application to black carbon particles. Global Biogeochem Cycles 2005;19(1):1013-25.

[2] Fowles M. Black carbon sequestration as an alternative to bioenergy. Biomass Bioenerg 2007;31(6):426-32.

[3] Laird DA. The charcoal vision: A win-win-win scenario for simultaneously producing bioenergy, permanently sequestering carbon, while improving soil and water quality. Agron J 2008;100(1):178-81.

[4] Jeffery S, Verheijen FGA, van der Velde M, Bastos AC. A quantitative review of the effects of biochar application to soils on crop productivity using meta-analysis. Agric Ecosyst Environ 2011;144(1):175-87.

[5] Baldock JA, Smernik RJ. Chemical composition and bioavailability of thermally altered *Pinus resinosa* (red pine) wood. Org Geochem 2002;33:1093-1109.

[6] Masiello CA, Druffel ERM, Currie LA. Radiocarbon measurements of black carbon in aerosols and ocean sediments. Geochem Cosmochim Acta 2002;66(6):1025-36.

[7] Cheng CH, Lehmann J, Thies JA, Burton SD, Engelhard MH. Oxidation of black carbon by biotic and abiotic processes. Org Geochem 2006;37:1477-88.

[8] Czimczik CI, Masiello CA. Controls on black carbon storage in soils. Global Biogeochem Cycles 2007;21:doi:10.1029/2006GB002798.

[9] Braadbaart F, Poole I, van Brussel AA. Preservation potential of charcoal in alkaline environments: an experimental approach and implications for the archaeological record. J Archaeol Sci 2009;36:1672-9.

[10] Nguyen BT, Lehmann J, Kinyangi J, Smernik R, Riha SJ, Engelhard MH. Long-term black carbon dynamics in cultivated soil. Biogeochem. 2009;92:163-76.

[11] Nocentini C, Certini G, Knicker H, Francioso O, Rumpel C. Nature and reactivity of charcoal produced and added to soil during wildfire are particle-size dependent. Org Geochem 2010;41:682-9.

[12] Zimmerman AR. Abiotic and microbial oxidation of laboratory-produced black carbon (biochar). Environ Sci Technol 2010;44(4):1295-1301.

[13] Peng X, Ye LL, Wang CH, Zhou H, Sun B. Temperature- and duration-dependent rice straw-derived biochar: characteristics and its effects on soil properties of an Ultisol in southern China. Soil Till Res 2011;112(2):159-66.

[14] Goldberg ED. Black Carbon in the Environment. New York: John Wiley and Sons; 1987.

[15] Hedges JI, Eglinton G, Hatcher PG, Kirchman DL, Arnosti C, Perenne S, et al. The molecularly-uncharacterized component of nonliving organic matter in natural environments. Org Geochem 2000;31:945-58.

[16] Masiello CA. New directions in black carbon organic geochemistry. Mar Chem 2004;92:201-13.

[17] Pastorova I, Botto RE, Arisz PW, Boon JJ. Cellulose char structure: a combined analytical Py-GC-MS, FTIR, and NMR study. Carbohydr Res 1994;262:27-47.

[18] Eckmeier E, Wiesenberg GLB. Short-chain *n*-alkanes ($C_{16–20}$) in ancient soil are useful molecular markers for prehistoric biomass burning. J Archaeol Sci 2009;36: 1590-6.

[19] Wiesenberg GLB, Lehndorff E, Schwark L. Thermal degradation of rye and maize straw: Lipid pattern changes as a function of temperature. Org Geochem 2009;40:167-74.

[20] Boon JJ, Pastorova I, Botto RE, Arisz PW. Structural studies on cellulose pyrolysis and cellulose chars by PYMS, PYGCMS, FTIR, NMR and by wet chemical techniques. Biomass Bioenerg 1994;7(1-6):25-32.

[21] Schneider MPW, Hilf M, Vogt UF, Schmidt MWI. Improved benzene polycarboxylic acid (BPCA) method to characterize char pyrolyzed between 200°C and 1000°C. Org Geochem 2010;41:1082-8.

[22] Ascough PL, Bird MI, Scott AC, Collinson ME, Cohen-Ofri I, Snape CE, et al. Charcoal reflectance measurements: implications for structural characterization and assessment of diagenetic alteration. J Archaeol Sci 2010;37:1590-9.

[23] Nguyen BT, Lehmann J, Hockaday WC, Joseph S, Masiello CA. Temperature sensitivity of black carbon decomposition and oxidation. Environ Sci Technol 2010;44(9):3324-31.

[24] Zimmerman AG, Gao B, Ahn MY. Positive and negative carbon mineralization priming effects among a variety of biochar-amended soils. Soil Biol Biochem 2011;43:1169-79.

[25] Maŝek O, Brownsort P, Cross A, Sohi S. Influence of biochar production conditions on its structure, properties and environmental stability. Fuel, in press, doi:10.1016/j.fuel.2011.08.044.

[26] Naafs DFW. What are humic substances? A molecular approach to the study of organic matter in acid soils [dissertation]: University of Utrecht; 2004, p. 99-106.

[27] Ross AB, Junyapoon S, Jones JM, Williams A, Bartle KD. A study of different soots using pyrolysis–GC–MS and comparison with solvent extractable material. J Anal Appl Pyrol 2005;74:494-501.

[28] De la Rosa JM. Aislamiento y caracterización de formas de materia orgánica refractaria en sedimentos marinos [dissertation]: Universidad de Sevilla; 2007. Spanish.

[29] Rumpel C, González-Pérez JA, Bardoux G, Largeau C, González-Vila FJ, Valentin C. Composition and reactivity of morphologically distinct charred materials left after slash-and-burn practices in agricultural tropical soils. Org Geochem 2007;38:911-20.

[30] De la Rosa JM, Knicker H, López-Capel E, Manning DAC, González-Pérez JA, González-Vila FJ. Direct detection of black carbon in soils by py-GC/MS, carbon-13 NMR spectroscopy and thermogravimetric techniques. Soil Sci Soc Am J 2008;72:258-67.

[31] Kaal J, Martínez Cortizas A, Reyes O, Soliño M. Molecular characterization of Ulex europaeus biochar obtained from laboratory heat treatment experiments - A pyrolysis-GC/MS study. J Anal Appl Pyrol 2012;95:205-12.

[32] Calvelo Pereira R, Kaal J, Camps-Arbestain M, Pardo Lorenzo R, Aitkenhead W, Hedley M, et al. Contribution to characterisation of biochar to estimate the labile fraction of carbon. Org Geochem 2011;42:1331-42.

[33] Fabbri D, Torri C, Spokas KA. Analytical pyrolysis of synthetic chars derived from biomass with potential agronomic application (biochar). Relationships with impacts on microbial carbon dioxide production. J Anal Appl Pyrol, in press, doi:10.1016/j.jaap.2011.09.012.

[34] Kaal J, Martínez Cortizas A, Nierop KGJ. Characterisation of aged charcoal using a coil probe pyrolysis-GC/MS method optimised for black carbon. J Anal Appl Pyrol 2009;85:408-16.

[35] Song J, Peng P. Characterisation of black carbon materials by pyrolysis-gas Chromatography-mass spectrometry. J Anal Appl Pyrol 2010;87:129-37.

[36]Schneider MPW, Smittenberg RH, Dittmar T, Schmidt MWI. Comparison of gas with liquid chromatography for the determination of benzenepolycarboxylic acids as molecular tracers of black carbon. Org Geochem 2011;42:275-82.

[37] McBeath AV, Smernik RJ, Schneider MWP, Schmidt MWI, Plant EL. Determination of the aromaticity and the degree of aromatic condensation of a thermosequence of wood charcoal using NMR. Org Geochem 2011;42:1194-202.

[38] Haefele SM, Knoblauch C, Gummert M, Konboon Y, Koyama S. Black carbon (biochar) in rice-based systems: characteristics and opportunities. In: Woods WI, Teixeira WG, Lehmann J, Steiner C, WinklerPrins AMGA, Rebellato L., editors. Amazonian Dark Earths: Wim Sombroek's Vision, Springer; 2009, p. 445-63.

[39] Haefele SM, Konboon Y, Wongboon W, Amarante S, Maarifat AA, Pfeiffer EM, et al. Effects and fate of biochar from rice residues in rice-based systems. Field Crop Res 2011;121(3):430-40.

[40] Hammes K, Smernik RJ, Skjemstad JO, Herzog A, Vogt UF, Schmidt MWI. Synthesis and characterisation of laboratory-charred grass straw (*Oryza sativa*) and chestnut wood (*Castanea sativa*) as reference materials for black carbon quantification. Org Geochem 2006;37:1629-33.

[41] Black Carbon Steering Committee. Black Carbon Reference Materials [cited 2012 April 11]. http://www.geo.uzh.ch/en/units/physical-geography-soilbio/services/black-carbon-reference-materials.

[42] Hammes K, Smernik RJ, Skjemstad JO, Schmidt MWI. Characterisation and evaluation of reference materials for black carbon analysis using elemental composition, colour, BET surface area and ^{13}C NMR spectroscopy. Appl Geochem 2008;23:2113-22.

[43] Di Blasi C, Branca C, Santoro A, González Hernández E. Pyrolytic behavior and products of some wood varieties. Combust Flame 2001;124:165-77.

[44] Keiluweit M, Nico PS, Johnson MG, Kleber M. Dynamic molecular structure of plant biomass-derived black carbon compounds (biochar). Environ Sci Technol 2010;44(4):1247-53.

[45] González-Vila FJ, Tinoco P, Almendros G, Martín F. Pyrolysis-GC-MS analysis of the formation and degradation stages of charred residues from lignocellulosic biomass. J Agric Food Chem 2001;49(3):1128-31.

[46] Pouwels AD, Eijkel GB, Boon JJ. Curie-point pyrolysis-capillary gas chromatography-high-resolution mass spectrometry of microcrystalline cellulose. J Anal Appl Pyrol 1989;14:237-80.

[47] Népo Murwanashyaka J, Pakdel H, Roy C. Step-wise and one-step vacuum pyrolysis of birch-derived biomass to monitor the evolution of phenols. J Anal Appl Pyrol 2001;60:219-31.

[48] Patwardhan PR, Satrio JA, Brown RC, Shanks BH. Influence of inorganic salts on the primary pyrolysis products of cellulose. Bioresour Technol 2010;101:4646-55.

[49] Nowakowski DJ, Jones JM. Uncatalysed and potassium-catalysed pyrolysis of the cell-wall constituents of biomass and their model compounds. J Anal Appl Pyrol 2008;83:12-25.

[50] Shafizadeh F, Lu YL. Pyrolysis of cellulose. Carbohydr Res 1973;29(1):113-22.

[51] Evans RJ, Milne TA. Molecular characterization of the pyrolysis of biomass. 1. Fundamentals. Energy Fuels 1987;1:123-37.

[52] Pastorova I, Arisz PW, Boon JJ. Preservation of D-glucose-oligosaccharides in cellulose chars. Carbohydr Res 2003;248:151-65.

[53] Almendros G, Dorado J, González-Vila FJ, Martin F. Pyrolysis of carbohydrate-derived macromolecules: its potential in monitoring the carbohydrate signature of geopolymers. J Anal Appl Pyrol 1997;40-41:599-610.

[54] Skjemstad JO, Clarke P, Taylor JA, Oades JM, McClure SG. The chemistry and nature of protected carbon in soil. Aust J Soil Res 1996;34(2):251-71.

[55] Knicker H, Totsche KU, Almendros G, González-Vila FJ. Condensation degree of burnt peat and plant residues and the reliability of solid-state VACP MAS ^{13}C NMR spectra obtained from pyrogenic humic material. Org Geochem 2005;36:1359-77.

[56] Kaal J, Rumpel C. Can pyrolysis-GC/MS be used to estimate the degree of thermal alteration of black carbon? Org Geochem 2009;40:1179-87.

[57] Saiz-Jiménez C., de Leeuw JW. Pyrolysis-gas chromatography-mass spectrometry of isolated, synthetic and degraded lignins. Org Geochem 1984;6;417-22.

[58] Schellekens J, Buurman P, Pontevedra-Pombal X. Selecting parameters for the environmental interpretation of peat molecular chemistry - a pyrolysis-GC/MS study. Org Geochem 2009;40:678-91.

[59] Saiz-Jiménez C. Analytical pyrolysis of humic substances: pitfalls, limitations, and possible solutions. Environ Sci Technol 1984;28(11):1773-80.

[60] Schnitzer MI, Monreal CM, Jandl G. The conversion of chicken manure to bio-oil by fast pyrolysis. III. Analyses of chicken manure, bio-oils and char by Py-FIMS and Py-FDMS. J Environ Sci Health, Part B 2008;43(1):81-95.

[61] Chechowski F, Marcinkowski T. Sewage sludge stabilisation with calcium hydroxide: effect on physicochemical properties and molecular composition. Water Res 2006;40(9):1895-1905.

[62] Knicker H, Almendros G, González-Vila FJ, Martin F, Lüdemann HD. ^{13}C- and ^{15}N-NMR spectroscopic examination of the transformation of organic nitrogen in plant biomass during thermal treatment. Soil Biol Biochem 1996;28:1053-60.

[63] Braadbaart F, Boon JJ, van der Horst J, van Bergen PF. Laboratory simulations of the transformation of peas as a result of heating: the change of the molecular composition by DTMS. J Anal Appl Pyrol 2004;71:997-1026.

[64] Smernik RJ, Baldock JA. Does solid-state ^{15}N NMR spectroscopy detect all soil organic nitrogen? Biogeochem. 2005;75(3):507-28.

[65] Knicker H. Pyrogenic organic matter in soil: its origin and occurrence, its chemistry and survival in soil environments. Quatern Int 2011;243(2):1-13.

[66] Knicker H. Soil organic N - An under-rated player for C sequestration in soils? Soil Biol Biochem 2011;43:1118-29.

[67] Lichtfouse É, Leblond C, Da Silva M, Behar F. Occurrence of biomarkers and straight-chain biopolymers in humin: implication for the origin of soil organic matter. Naturwissenschaften 1998;85(10):497-501.

[68] Ishiwatari M, Ishiwateri R, Sakashita H, Tatsumi T, Tominaga H. Pyrolysis of chlorophyll a after preliminary heating at a moderate temperature: implications for the origin of prist-l-ene on kerogen pyrolysis. J Anal Appl Pyrol 1991;18;207-18.

[69] Kaal J, Brodowski S, Baldock JA, Nierop KGJ, Martínez Cortizas A. Characterisation of aged black carbon using pyrolysis-GC/MS, thermally assisted

hydrolysis and methylation (THM), direct and cross polarisation ^{13}C nuclear magnetic resonance (DP/CP NMR) and the benzenepolycarboxylic acid (BPCA) method. Org Geochem 2008;39:1415-26.

[70] Czimczik CI, Preston CM, Schmidt MWI, Werner RA, Schulze ED. Effects of charring on mass, organic carbon, and stable carbon isotope composition of wood. Org Geochem 2002;33:1207-23.

[71] Knicker H, González-Vila FJ, Polvillo O, González-Pérez JA, Almendros G. Fire-induced transformation of C- and N- forms in different organic soil fractions from a Dystric Cambisol under a Mediterranean pine forest (*Pinus pinaster*). Soil Biol Biochem 2005;37:701-18.

[72] Amen-Chen C, Pakdel H, Roy R. Production of monomeric phenols by thermochemical conversion of biomass: a review. Bioresour Technol 2001;79(3):277-9.

[73] Ohara S, Yasuta Y, Ohi H. Structure elucidation of condensed tannins from barks by pyrolysis/gas chromatography. Holzforschung 2003;57(2):145-9.

[74] Di Blasi C, Branca C, Santoro A, Perez Bermudez RA. Weight loss dynamics of wood chips under fast radiative heating. J Anal Appl Pyrol 2001;57:77-90.

[75] Rushdi AI, Ritter G, Grimalt JO, Simoneit BRT. Hydrous pyrolysis of cholesterol under various conditions. Org Geochem 2003;34:799-812.

[76] Ziolkowski LA, Druffel ERM. Aged black carbon identified in marine dissolved organic carbon. Geophys Res Lett 2010;37:L16601.

[77] Ascough PL, Bird MI, Francis SM, Thornton B, Midwood AJ, Scott AC, et al. Variability in oxidative degradation of charcoal: Influence of production conditions and environmental exposure. Geochim Cosmochim Acta 2011;75(9):2361-78.

[78] Bruun S, Jensen ES, Jensen LS. Microbial mineralization and assimilation of black carbon: Dependency on degree of thermal alteration. Org Geochem 2008;39:839-45.

[79] Ziolkowski LA, Chamberlin AR, Greaves J, Druffel ERM. Quantification of black carbon in marine systems using the benzene polycarboxylic acid method: a mechanistic and yield study. Limnol Oceanogr 2011;9:140-9.

TABLES

	mass recovery [% of initial]	C [mass-%]	H [mass-%]	N [%] [mass-%]	O [%] [mass-%]	H/C (atomic)* [-]	O/C (atomic) [-]	N/C (atomic) [-]
Chestnut wood								
200	88.0	50.3	5.6	0.1	44.2	1.33	0.66	0.002
250	71.0	54.3	5.3	0.1	40.1	1.16	0.55	0.002
275	52.5	64.1	4.3	0.2	31.4	0.80	0.37	0.002
300	44.8	69.5	4.0	0.2	26.1	0.69	0.28	0.002
350	41.0	73.4	3.2	0.3	23.0	0.52	0.24	0.003
400	31.0	78.1	3.0	0.3	18.5	0.46	0.18	0.003
500	30.7	87.1	2.7	0.3	9.8	0.36	0.08	0.003
600	25.5	93.8	1.9	0.3	3.9	0.24	0.03	0.003
700	27.5	95.1	1.1	0.5	3.3	0.14	0.03	0.004
800	27.0	96.0	0.7	0.7	2.4	0.08	0.02	0.006
900	25.0	96.5	0.3	0.8	2.2	0.04	0.02	0.007
1000	27.0	96.3	0.2	1.0	2.5	0.03	0.02	0.009
Rice straw								
200	86.0	46.2	5.4	0.8	39.2	1.39	0.64	0.016
250	62.8	52.1	5.2	0.9	32.5	1.19	0.47	0.016
275	49.0	58.5	4.6	1.4	24.3	0.95	0.31	0.020
300	45.3	59.2	4.3	1.1	22.7	0.87	0.29	0.015
350	39.4	62.1	3.6	1.2	20.0	0.70	0.24	0.016
400	35.0	63.1	3.0	1.0	16.2	0.58	0.19	0.013
500	32.2	66.8	2.3	0.9	11.3	0.41	0.13	0.011
600	33.0	67.4	1.5	0.8	9.6	0.27	0.11	0.010
700	27.9	69.8	1.1	0.8	11.6	0.18	0.12	0.010
800	27.1	66.6	0.8	1.1	9.8	0.14	0.11	0.014
900	23.8	71.0	0.5	0.9	9.1	0.08	0.10	0.010
1000	21.9	72.1	0.3	0.7	7.0	0.05	0.07	0.008

Table 1: Mass recovery and elemental composition data for chestnut wood and rice straw charred between 200 and 1000 °C (T_{CHAR}). *Data from Schneider et al. [36].

FIGURES

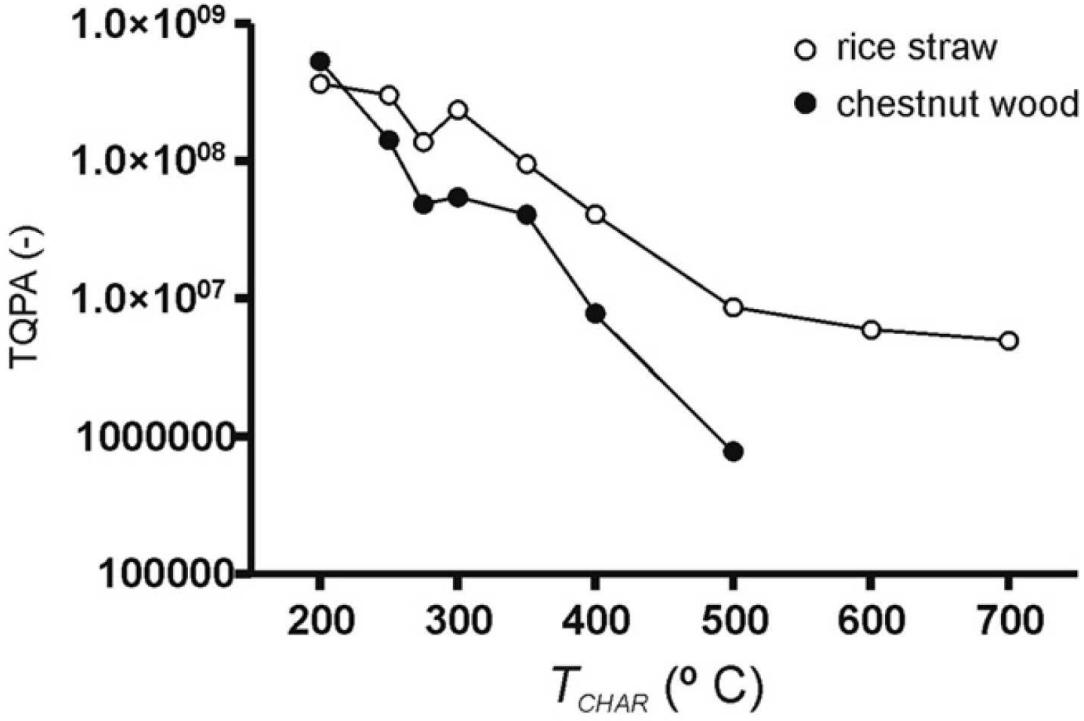

Figure 1: Relation between charring temperature (T_{CHAR}) and pyrolysis-GC/MS signal intensity (total quantified peak area, TQPA) for rice straw and chestnut wood.

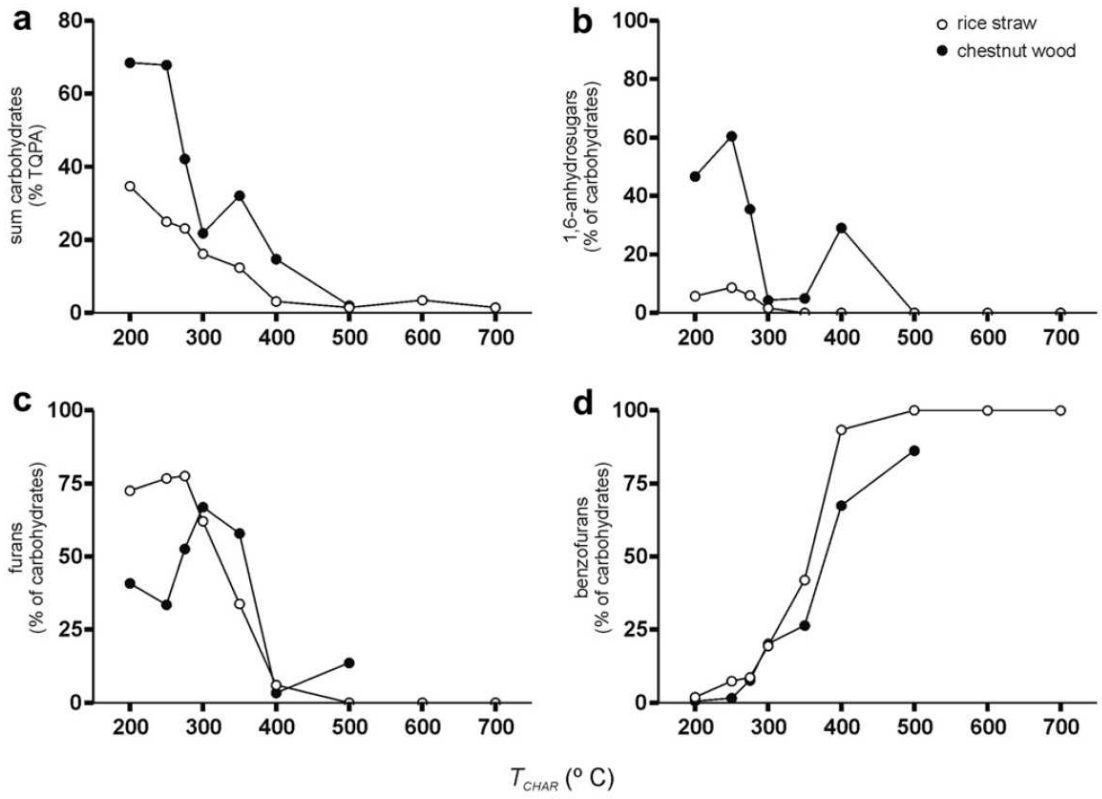

Figure 2: The relative proportions (as % of TQPA) of a) the sum of carbohydrate markers, b) 1,6-anhydrosugars, c) furans and furaldehydes and d)benzofurans, plotted against T_{CHAR}.

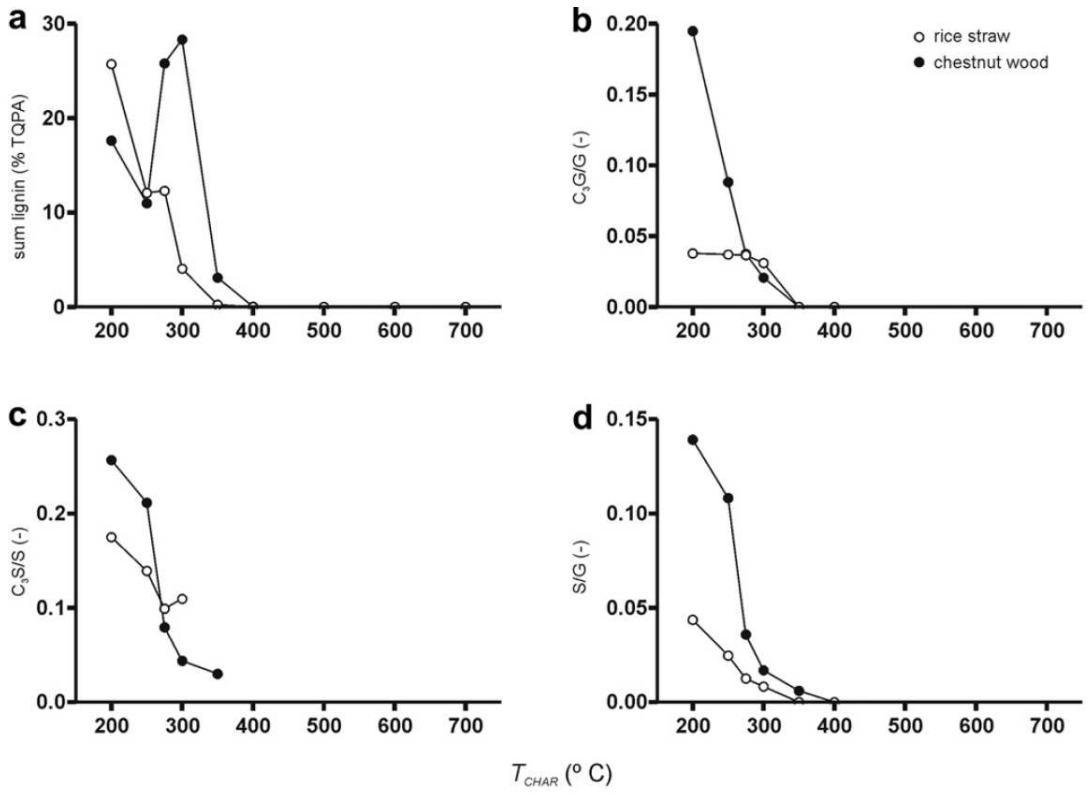

Figure 3: a) The relative proportion (as % of TQPA) of the sum of lignin markers, plotted against T_{CHAR}. Pyrolysis product ratios b) C_3-guaiacols/guaiacols (C_3G/G), c) C_3-syringols/syringols (C_3S/S) and d) syringols/guaiacols (S/G).

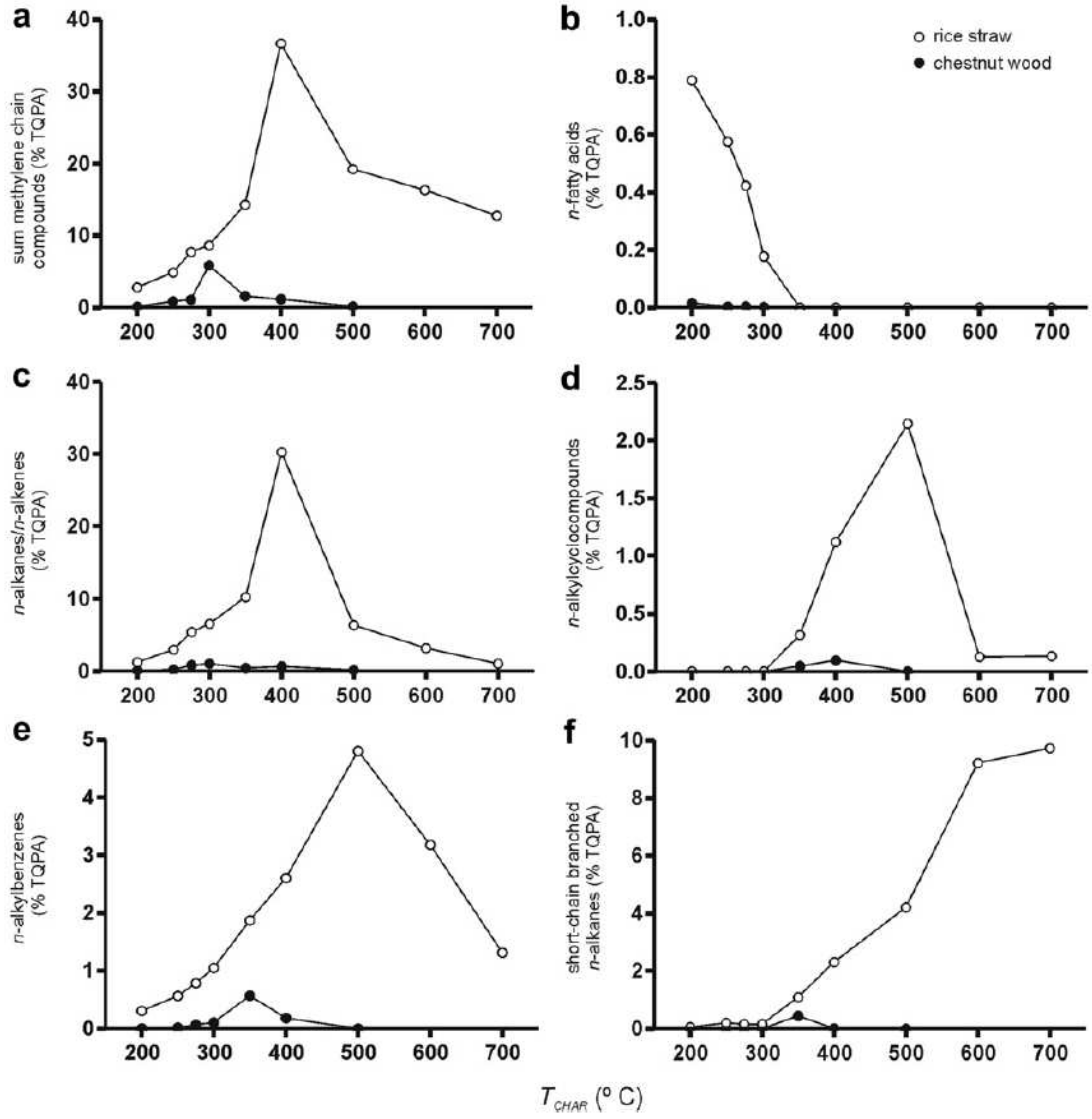

Figure 4: The relative proportions (as % of TQPA) of a) the sum of methylene chain compounds, and subgroups: b) *n*-fatty acids, c) C_{11}-C_{33} alkanes/*n*-alkenes, d) *n*-alkylcyclocompounds, e) *n*-alkylbenzenes and f) short-chain *n*-alkanes, plotted against T_{CHAR}.

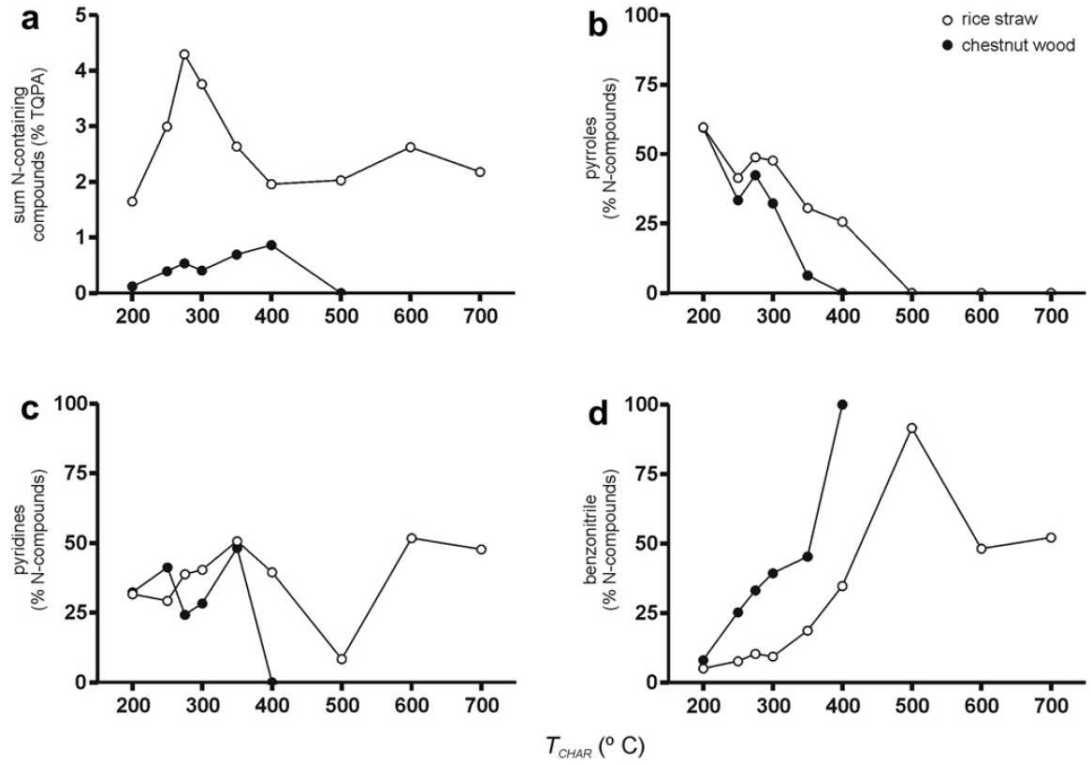

Figure 5: The relative proportions (as % of TQPA) of a) the sum of N-containing pyrolysis products, b) pyrroles, c) pyridines and d) benzonitrile,plotted against T_{CHAR}.

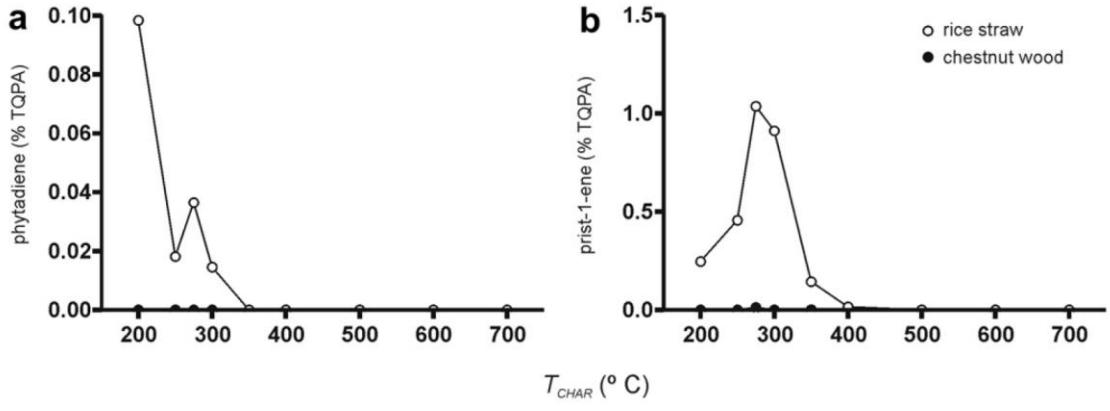

Figure 6: The relative proportions (as % of TQPA) of a) phytadiene and b) prist-1-ene, plotted against T_{CHAR}.

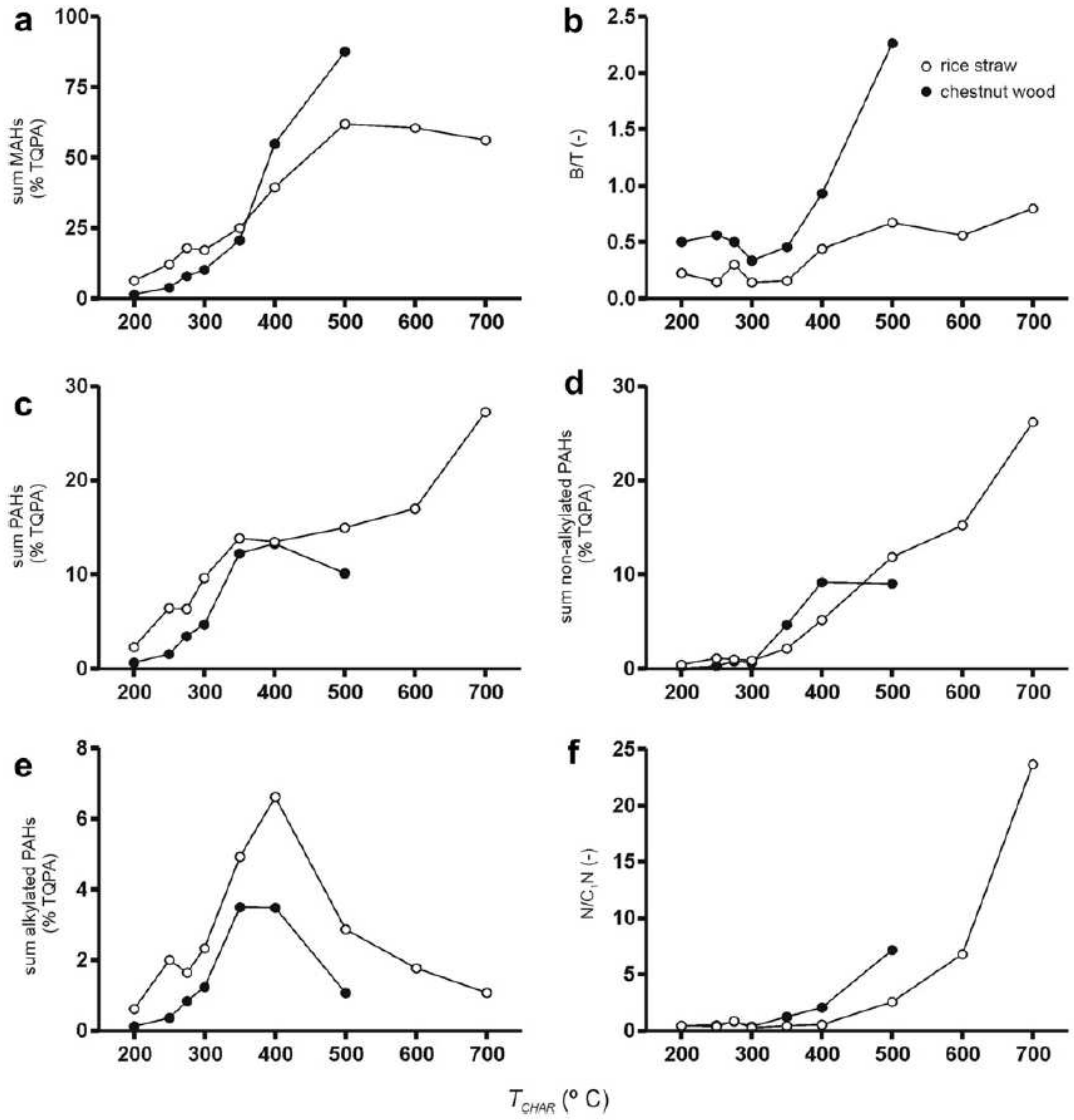

Figure 7: The relative proportions (as % of TQPA) of a) monocyclic aromatic hydrocarbons (MAHs), c) polycyclic aromatic hydrocarbons (PAHs), d) non-alkylated PAHs and e) alkylated PAHs, plotted against T_{CHAR}. Pyrolysis product ratios: b) benzene-to-toluene (B/T) and f) naphthalene-to-C_1-naphthalenes (N/C_1N) ratios, plotted against T_{CHAR}.

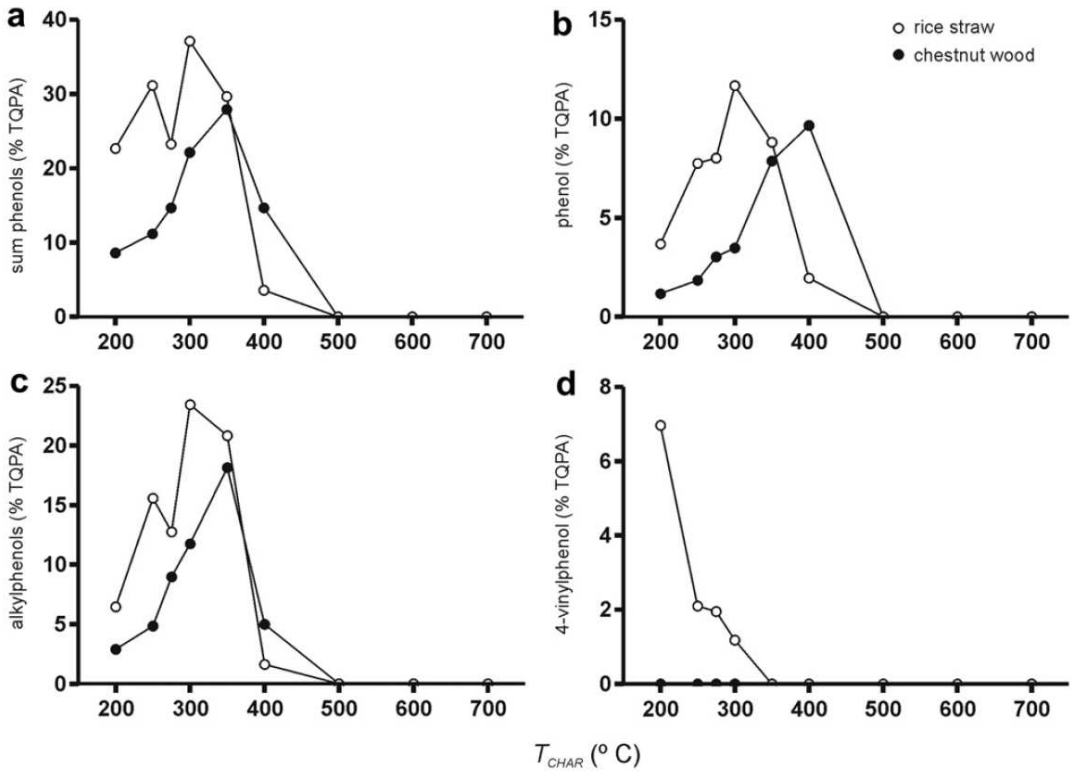

Figure 8: The relative proportions (as % of TQPA) of a) the sum of phenols, b) phenol, c) C_1-C_3 alkylphenols and d) 4-vinylphenol plotted against T_{CHAR}.

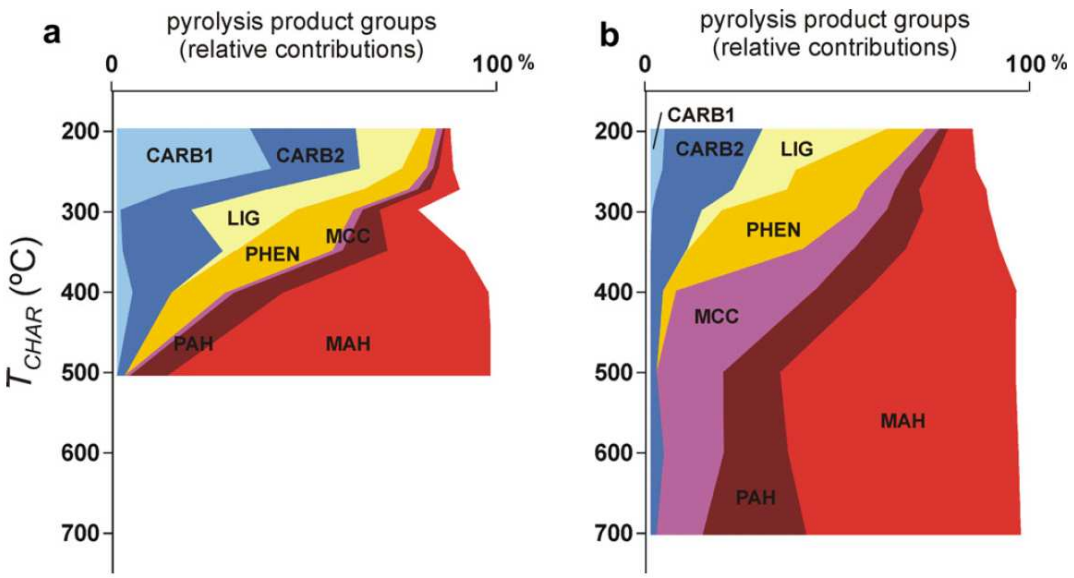

Figure 9: Summary of changes in pyrolysis fingerprint upon heat treatment (T_{CHAR} 200-700 °C) of a) chestnut wood thermosequence and b) rice straw thermosequence. Abbreviations: CARB1 = anhydrosugars, pyrans; CARB2 = other carbohydrate products; LIG = lignin (4-vinylphenol, guaiacols, syringols); PHEN = phenols; MCC = methylene chain compounds; PAH = polycyclic aromatic hydrocarbons, MAH = monocyclic aromatic hydrocarbons.

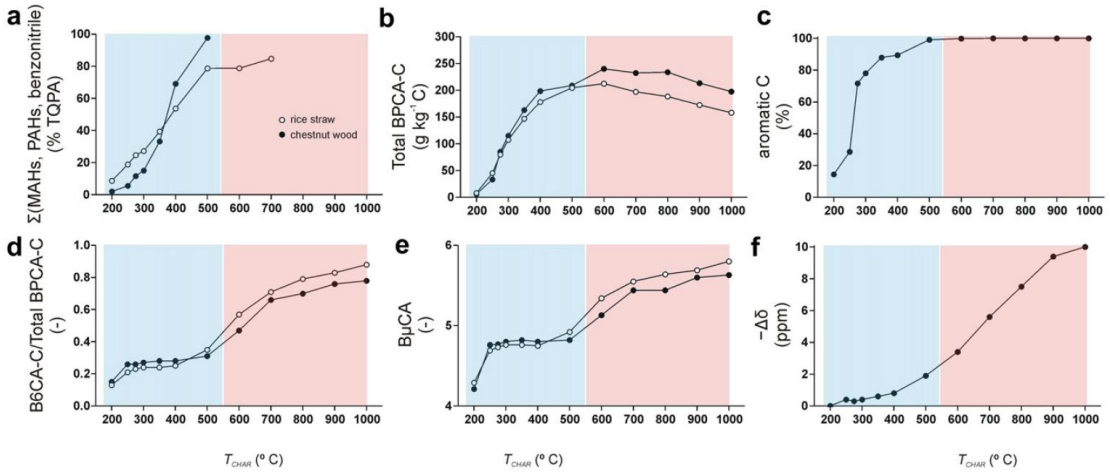

Figure 10: Parameters used for estimating Black C content, plotted against T_{CHAR}: a) Σ(MAHs, PAHs, benzonitrile) from pyrolysis-GC/MS, b) Total BPCA from the BPCA method and c) % aromatic C from ^{13}C DP NMR. Parameters used for estimating the charring intensity of Black C: d) the proportion of B6CA among all BPCA (B6CA-C/Total BPCA-C), e) the average number of acidic groups in the BPCA (BμCA) and f) chemical shift change of Black C-bound ^{13}C benzene (-Δδ, from ring current NMR). Results of BPCA method modified after [36] (Fig. 5b, using HPLC/DAD) and results of NMR from [37].